ACCURACY OF TIME INTEGRATION PROCEDURES FOR SEISMIC RESPONSE OF LINEAR OSCILLATORS

J. Arias[1] and R. Blázquez[2]

[1] *Research Assistant, Dept. of Civil Engr. and Construction, Univ. de Castilla-La Mancha, Ciudad Real. Spain.*
[2] *Professor, Dept. of Civil Engr. and Construction, Univ. de Castilla-La Mancha, Ciudad Real .Spain*
Email: Juana.Arias@uclm.es , Rafael.Blazquez@uclm.es

ABSTRACT :

The goodness of time integration algorithms commonly used in earthquake engineering is characterized in this paper by the ratios of their transfer function to the ones corresponding to the exact integration operator. This approach permits to appraise very easily how the different components of the seismic action are affected by the oscillator and to quantify the adequacy of the integration scheme as the excitation frequency approaches the Nyquist frequency. Using this methodology, the effects of various temporal algorithms (recursive digital filters) on the accuracy of the seismic response of linear systems are investigated, both for Duhamel integral methods and for time-stepping methods. Analytical solutions are applied to several examples of discrete and continuum linear systems to elucidate the influence on the overall error of the unknown variation of the input motion between sampling points, as well as the uneven distortion of the frequencies introduced by the integration process.

KEYWORDS: Temporal integration, transfer functions, dynamics of linear oscillators, Nyquist frequency.

1. INTRODUCTION

Generally speaking, time integration algorithms are nothing else but linear combinations of the numerical data (base points, t_i, and function to be integrated, $x(t_i)$), derived from polynomial approximations of the function $x(t_i)$, either for equidistant points (Newton-Cotes methods) or for points located at non-equal time intervals (Gaussian quadrature methods). In this paper, we restrict the analysis to four well known integration methods of the first category, namely the trapezoidal, Simpson's, rectangle and mid-point rules, which are shown schematically in Fig. 1.

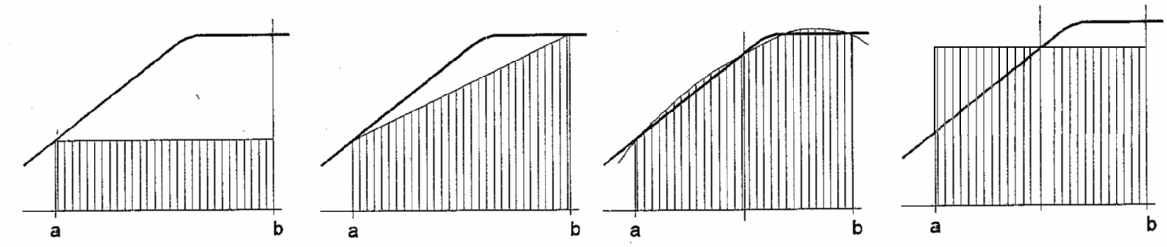

Figure 1.- Quadrature rules: a) rectangle; b) trapezoidal; c) Simpson's; d) mid-point

The mathematical formulation of these four methods is indicated in Table 1.1:

Table 1.1

Trapezoidal rule	**Simpson's rule**
$y_{n+1} = y_n + \frac{h}{2}(x_n + x_{n+1});\ n = 0,1,2,...$ (1.1)	$y_{n+1} = y_{n-1} + \frac{h}{3}(x_{n-1} + 4x_n + x_{n+1});\ n = 1,2,3...$ (1.2)
Rectangle rule	**Mid-point rule**
$y_{n+1} = y_n + hx_n;\ n = 0,1,2,...$ (1.3)	$y_{n+1} = y_n + hx_{n+1/2};\ n = 0,1,2,...$ (1.4)

where $h = t_j - t_i \ \ (j > i)$, and $y(t) = \int x(t)dt$ (1.5)

Since this research focuses on seismic signals, rapidly varying with time, it is important to analyze the frequency response of the above integration rules, in order to elucidate the distortion introduced by them in the frequency content of the signals being integrated.

2. TRANSFER FUNCTIONS OF QUADRATURE RULES

The integration schemes of Eqs. 1.1 - 1.4 can be characterized as recursive digital filters of causal type with memory. Therefore, according to Hamming (1977), their degree of accuracy for a given frequency can be estimated by computing the ratio between the transfer function of the numerical (approximate) and the analytical (exact) temporal operators. To do so, an input complex harmonic signal, $e^{i\omega t}$, is assumed. Since the above equations are all linear, the output signal after integration will be of the type $H(i\omega)e^{i\omega t}$, where $H(i\omega)$ is the complex transfer function of the integrator and ω is the angular frequency (Fig. 2).

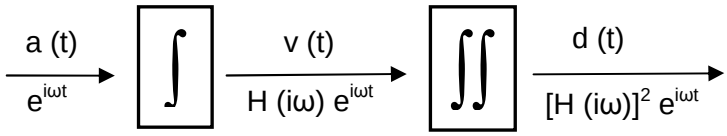

Figure 2.- Transfer functions of time integration operators applied to a seismic acceleration record

Then, for the ideal integrator it is found

$$H^*(i\omega)e^{i\omega t} = y(t) = \int e^{i\omega t}dt = \frac{e^{i\omega}}{i\omega} \qquad (2.6)$$

$$H^*(i\omega) = \frac{1}{i\omega}e^{-i\pi/2} \Rightarrow \left|H^*(i\omega)\right| = \frac{1}{\omega};\ \ \phi^*(i\omega) = -\frac{\pi}{2} \qquad (2.7)$$

whereas for the quadrature rules, making $x_n = e^{i\omega nh}$ and $y_n = H(i\omega)x_n$ in Eqs. 1.1-1.4, the expressions of Table 1.2 are derived (n=number of sampling points; h=Δt=discretization time interval).

Table 2.2

Trapezoidal rule	**Simpson's rule**
$H(i\omega) = \frac{h}{2}\cot(\frac{wh}{2})e^{-i\frac{\pi}{2}}$ (2.8)	$H(i\omega) = \frac{h}{3}\frac{2+\cos(\omega h)}{\sin(\omega h)}e^{-i\frac{\pi}{2}}$ (2.9)
Rectangle rule	**Mid-point rule**
$H(i\omega) = \frac{h}{2\cdot\sin(\frac{\omega h}{2})}e^{-i\left(\frac{\pi}{2}+\frac{\omega h}{2}\right)}$ (2.10)	$H(i\omega) = \frac{h}{2\cdot\sin(\frac{\omega h}{2})}e^{-i\frac{\pi}{2}}$ (2.11)

The moduli of the complex-variable functions 2.8 – 2.11, normalized with respect to that of the ideal integrator (Eqn. 2.7), are represented in Fig. 3-a, and the corresponding normalized phases angles are drawn in Fig. 3-b. In both diagrams $\omega_N=\pi/h$ is the so-called circular Nyquist frequency, which is the maximum frequency that can be reached if "aliasing" effects are to be avoided. From the inspection of Fig. 3, the following observations are made:

1) The rectangle, mid-point and Simpson's formulae amplify the amplitude of the signals throughout the whole frequency range (especially for harmonics above one-half of Nyquist frequency), whereas the trapezoidal rule attenuates progressively all the frequencies in the interval (0, ω_N).

2) The rectangle rule (also called "simple summation rule") is the only one that introduces a frequency-dependent phase shift in the integration process which leads to baseline drifts and distortions in the shape of the integrated signal (Fig. 3-b). Consequently, the use of the rectangle rule is not recommended for solving earthquake problems in engineering practice.

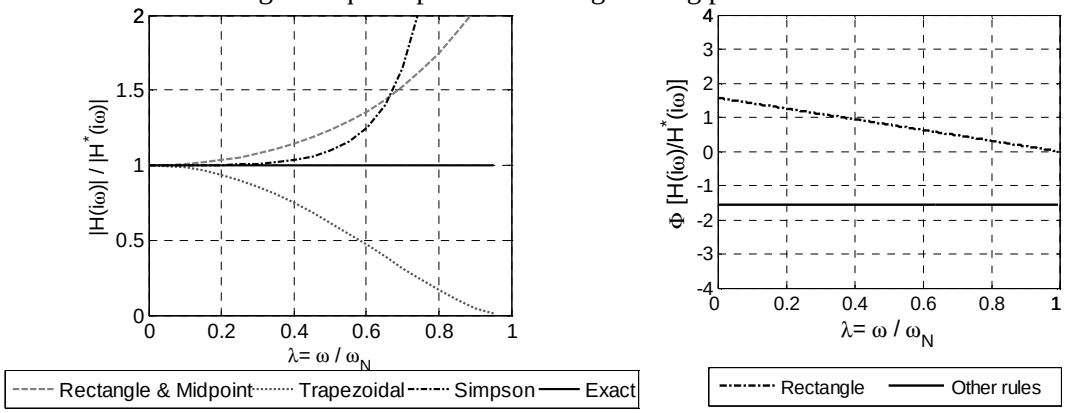

a) b)

Figure 3.- Normalized transfer functions of quadrature rules: a) amplitude values; b) phase angles

The practical implications of the above behavioral patterns are quite evident. Consider, for example, the simulated accelerogram proposed in the literature by Bogdanoff et al (1961)

$$\ddot{y}(t) = Bte^{\alpha t}\sum_{j=1}^{n}\cos(\omega_j t + \phi_j) \qquad (2.12)$$

with B=0.292 and α=-0.333; *n* is the number of harmonics with circular frequencies ω_j considered in the simulation, and Φ_j are random numbers uniformly distributed between 0 and 2π (Table 2.3).The artificial accelerogram (2.12) is analytically integrable all the way up to the response spectra, thus permitting to calibrate very easily the effectiveness and accuracy of several integration methods currently employed in earthquake engineering. Besides, by choosing adequately the parameters *n* and ω_j , the frequency content of the signal can be controlled at will.

Table 2.3

ω_j (rad/sec)	6.00	8.00	10.00	11.15	12.30	13.25	14.15	16.20	17.35	19.15	22.00
ϕ_j (rad)	3.7663	1.3422	4.8253	0.2528	4.5204	1.8834	1.3320	1.7852	0.1517	2.4881	1.7654
ω_j (rad/sec)	25.25	29.85	34.50	39.60	46.45	53.00	58.60	66.75	71.15	74.80	80.25
ϕ_j (rad)	1.6632	2.1862	0.8325	1.2387	2.3156	3.0012	1.0645	0.7843	1.5532	0.9586	2.3562

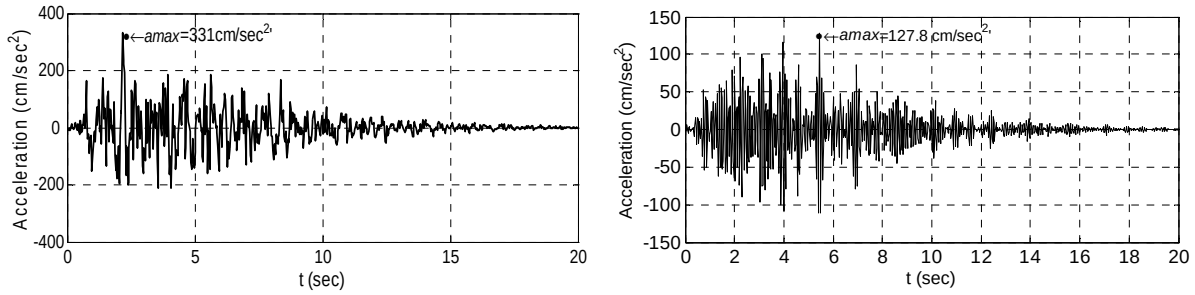

a) b)

Figure 4.-Simulated accelerograms (Bogdanoff et al, 1961): a) standard; b) enriched in high frequencies.

Thus, Figure 4-a depicts the simulated accelerogram, for *n*= 22, and 6.00< ω_i < 80.25 rad/sec. On the other hand, in Fig. 4-b, *n*= 5, and 58.60< ω_i < 80.25 rad/sec. Integrating the accelerogram of Fig. 4-b by means of the Simpson's and trapezoidal rules, with h =0.025 sec (40 sample points per second), gives the diagrams of Figs. 5-b and 5-c, while the exact velocigram is represented in Fig. 5-a. It becomes obvious how the trapezoidal rule truncates the high frequency peaks of the integrated signal whereas the Simpson's rule magnifies those peaks, an undesirable deleterious effect if spurious noise due to poor processing of the signal is to be expected.

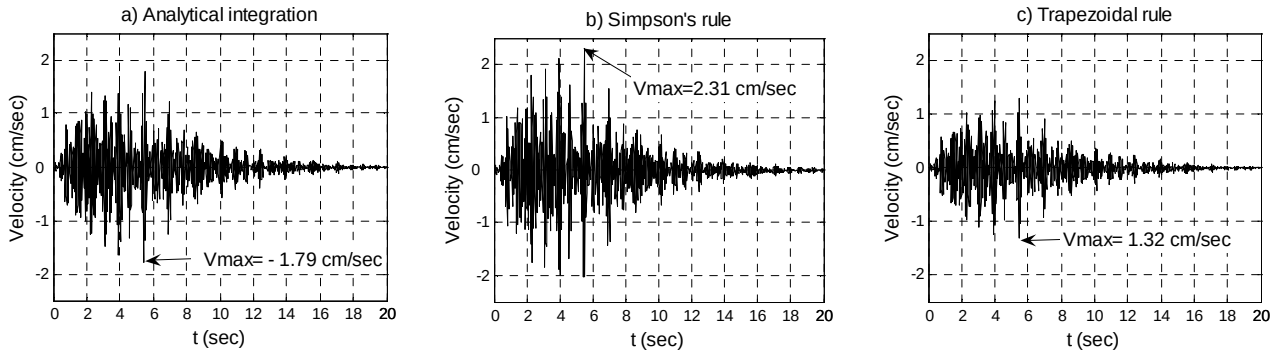

Figure 5.- Analytical a) vs. numerical integration [b) and c)] of the accelerogram shown in Fig. 4-b

3. SEISMIC RESPONSE OF 1 D.O.F. LINEAR SYSTEMS

3.1. Time-history analysis

The evaluation of the seismic response of a mass-spring-dashpot system subjected to an input base acceleration, $\ddot{y}(t)$, requires to solve the classical second-order ordinary differential equation

$$\ddot{u} + 2\xi p\dot{u} + p^2 u = -\ddot{y}(t) \qquad (3.13)$$

where $p=2\pi/T_n$ is the natural frequency of the oscillator, ξ is the damping ratio and $u, \dot{u}, \ddot{u}$ stand for the relative displacement, relative velocity, and relative acceleration of the oscillator. Assuming that the initial displacement and the initial velocity of the system are zero ("at rest" conditions at zero time), two possible methods are available in the literature for solving Eqn. 3.13:

- Direct integration of the differential equation (3.13), by numerical calculation of the so-called convolution integral or Duhamel's integral

$$u\ (t) = -\frac{1}{p_d}\int_0^t \ddot{y}(\tau) e^{-\xi p(t-\tau)} \sin[p_d(t-\tau)]d\tau \qquad (3.14)$$

- Step-by-step integration of Eqn 3.13, following a matricial marching scheme of the type

$$\begin{Bmatrix} u_{n+1} \\ \dot{u}_{n+1} \end{Bmatrix} = A(p,\xi)\begin{Bmatrix} u_n \\ \dot{u}_n \end{Bmatrix} + B(p,\xi)\begin{Bmatrix} \ddot{y}_n \\ \ddot{y}_{n+1} \end{Bmatrix} \qquad (3.15)$$

In both cases, the accuracy analysis is based in the comparison between the numerical transfer functions of u and $\dot{u}$ and the corresponding values for the exact integration of Eqn. 3.13. It must be remarked that this procedure differs substantially from the classical error analysis based on the amplitude decay and period elongation of the free response of the undamped system to an initial displacement (Humar,1990). Such an analysis considers only the matrix A (which governs the stability of the method), and does not take into account the forced terms of Eqn. 3.15 (Preumont, 1982).

The transfer functions of a linear system are frequency operators which characterize the ratio between the kinematic responses of the system and the corresponding excitations in the frequency domain. The accuracy of these complex-variable functions depends largely on the numerical method used to calculate the response of the system, as it is shown next.

a) Exact transfer functions

Substituting in Eqn. 3.13: $\ddot{y}(t) = e^{i\omega t}$; $u(t) = H_u^*(i\omega)e^{i\omega t}$; $\dot{u}(t) = H_{\dot{u}}^*(i\omega)e^{i\omega t} = i\omega H_u^*(i\omega)e^{i\omega t}$; $\ddot{u}(t) = -\omega^2 H_u^*(i\omega)e^{i\omega t}$, the following expressions for the stationary response are found (Fig. 6)

$$H_u^*(i\omega) = \frac{1}{\omega^2 - p^2 - 2i\xi\omega p} \qquad (3.16)$$

$$H_{\dot{u}}^*(i\omega) = i\omega H_u^*(i\omega\xi) \qquad (3.17)$$

$$H_{\ddot{x}}^*(i\omega) = -2\xi p H_{\dot{u}}^*(i\omega) - p^2 H_u^*(i\omega) \qquad (3.18)$$

where $\ddot{x}(t) = \ddot{u}(t) + \ddot{y}(t)$ denotes the absolute acceleration of the oscillator.

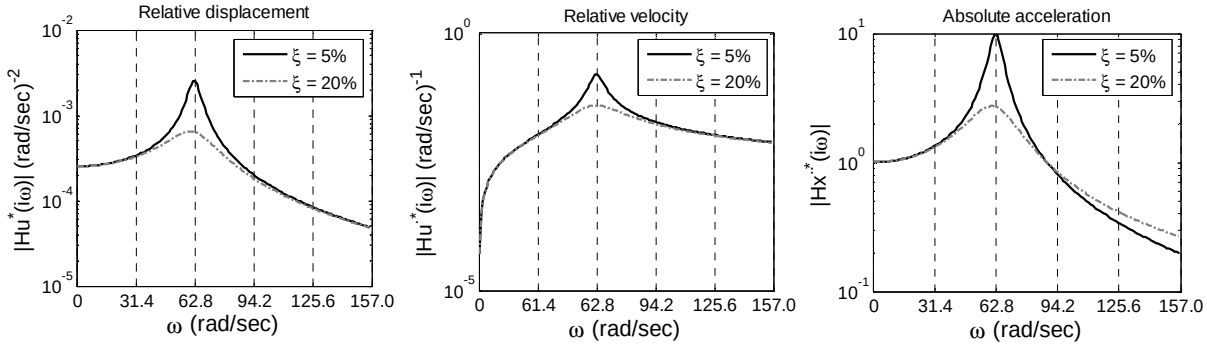

Figure 6.- Moduli of the exact transfer functions of short period oscillator (T_n=0.1 sec).

b) Numerical transfer functions: Duhamel's approach

In this method the numerical errors are due solely to the amplitude of the integration interval, h (assumed in this work identical to the digitization interval), and/or the hypothesis made about the variation of the excitation, $\ddot{y}(t)$, between sampling points (Blázquez and Arcos, 1999a). In all cases the transfer functions will be limited to the uppermost value of the frequency: $\omega_N = \pi / h$ (Nyquist frequency) to prevent "aliasing phenomena".

Then, for a resting system, substituting in Eqn. 3.13 $\ddot{y}(\tau) = e^{i\omega\tau}$, and developing the integral, gives

$$H_u(i\omega,t) = \frac{H^2(i\omega)}{1 + 2\xi p H(i\omega) + p^2 H^2(i\omega)}\left[1 - e^{-(p\xi + i\omega)t}\left(\cos(p_d t) + \frac{1 + \xi p H(i\omega)}{p_d H(i\omega)}\sin(p_d t)\right)\right] \qquad (3.19)$$

A similar expression has been derived by Lin (1967), for the stochastic response of a linear system to a weakly stationary random excitation, using a completely different approach. Note that $H_u(i\omega,t)$ is a non-stationary transfer function whose amplitude evolves with time, according to the transient nature of the seismic action (Fig. 7). As expected, when $t \rightarrow \infty$ the expression in brackets in Eqn 3.19 tends to unity, meaning that the stationary vibration phase has been reached. Under these conditions, substituting for example $H(i\omega)$ by

$H^*(i\omega)$ in Eqn 3.19, the value of the exact transfer function of u(t) for the analytical integration, $H_u^*(i\omega)$, is obtained. This procedure applies to any integration rule used in conjunction with Eqn 3.19. Figs. 8-a and 8-b exemplify this methodology for the Duhamel-trapezoidal and Duhamel-Simpson methods applied to two 5% damped oscillators with natural periods 0.1 and 5 sec. It can be seen in the figure that the opposite amplification trends of the two quadrature rules (Fig 3-a) mark the behavior of the respective transfer functions outside the resonance band of the system.

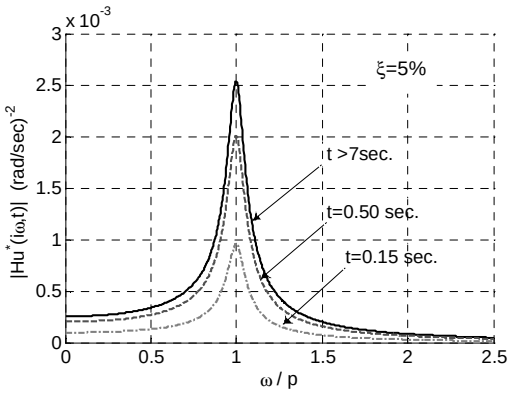

Figure 7.- Evolutionary transfer function amplitudes of the relative displacement of a 1 D.O.F. system at the transient (t < 7sec) and stationary (t ≥7sec) phases.

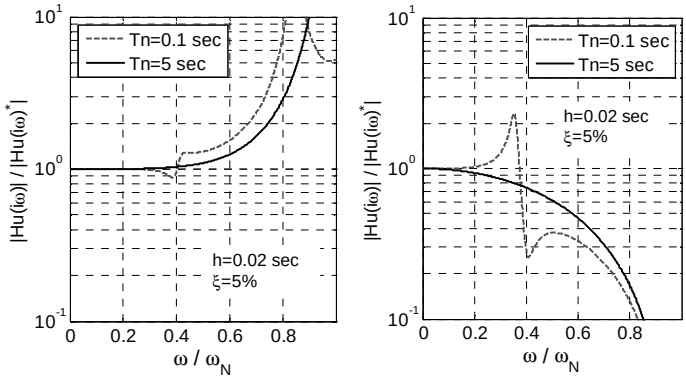

a) b)

Figure 8.- Normalized displacement transfer function diagrams for a 5%-damped system: (a) Duhamel–Simpson rule, (b) Duhamel-trapezoidal rule (Blázquez, 2007).

c) Numerical transfer functions: step-by-step integration algorithms

The way to proceed using this approach (Blázquez and Arcos, 1999b) is to derive the functions $H_u(i\omega,h), H_{\dot{u}}(i\omega,h)$ else solving the matricial Eqn. 3.15 as follows (n=number of sampled input values; I=unity matrix)

$$u_n = H_u(i\omega,h)e^{i\omega nh};\ \ \dot{u}_n = H_{\dot{u}}(i\omega,h)e^{i\omega nh} \qquad (3.20)$$

$$\begin{Bmatrix} H_u(i\omega,h) \\ H_{\dot{u}}(i\omega,h) \end{Bmatrix} = \left[e^{i\omega nh}I - A(p,\xi)\right]^{-1} B(p,\xi)\begin{Bmatrix} 1 \\ e^{iwnh} \end{Bmatrix} \qquad (3.21)$$

or directly, from the mathematical scheme which defines the integration algorithm. For example, for the central difference method (Newmark γ=1/2; β=0 method),

$$\dot{u}_n = \frac{1}{2h}(u_{n+1} - u_{n-1});\quad \ddot{u}_n = \frac{u_{n+1} - 2u_n + u_{n-1}}{h^2} \qquad (3.22)$$

substituting in Eqn. 3.13, written in discrete form, the quantities: $u_n = H_u e^{i\omega nh}$; $u_{n-1} = H_u e^{i\omega(n-1)h}$; $u_{n+1} = H_u e^{i\omega(n+1)h}$; $\ddot{y}_n = e^{i\omega nh}$, it results

$$H_u(i\omega,h) = \frac{1}{2 - p^2 - 2\left(\cos(\omega h) + i\frac{\xi p}{h}\sin(\omega h)\right)} \qquad (3.23)$$

which is the seismic transfer function of the method, strongly dependent on the amplitude of the integration interval, h.

Note that Eqs 3.20, 3.21 and 3.23 apply only to time-invariant conditions – that is when the transient phase of the forced vibration response has vanished- whereas Eqn. 3.19 is valid for the transient and stationary phases, in spite of the fact that the latter is not always reached during seismic loading. Note also that, for the operators H_u and $H_{\dot{u}}$ being applicable in practice, they must comply with the consistency conditions

$$H_u(0) = H_u^*(0); \quad H_{\dot{u}}(0) = i\omega H_{\dot{u}}^*(0) \qquad (3.24)$$

as well as with the standard requirements of stability and convergence of the method.

In this research, the performance of fourteen time stepping methods has been investigated, including three Runge-Kutta methods (2nd, 3rd and 4th order), five Newmark γ=1/2 methods (β=0, β=1/4, β=1/6, β=1/8, and β=1/12), three modified Newmark methods (HHT, WBZ and CH), and the Nigam-Jennings, Wilson θ and Houbolt methods. Fig. 9 shows the normalized transfer functions of the displacement, velocity and acceleration of short and long period damped oscillators calculated using three of the above methods, namely the Nigam-Jennings (N-J), Houbolt and central difference methods. It is realized from the figure that the N-J method behaves smoothly throughout the whole range of frequencies, deamplifying lightly the response to high and low frequencies for all types of oscillators. On the contrary, the other two methods show a strong resonance peak for all kinematic responses, diverging significantly from the exact ones in that zone. Furthermore, Fig. 9 confirms that, whereas the central difference method amplifies dangerously the excitation frequencies higher than the natural frequencies, Houbolt's method filters those frequencies, which are not accurately integrated and, consequently, are damped out in the response. This "numerical damping" effect is inherent to several integration methods (e.g. Wilson θ), and acts similarly to modal truncation in the frequency domain analysis of multi-degree-of-freedom systems, leading ultimately to attenuated spectral ordinates in the high frequency region. In practical computations, the presence of numerical damping is convenient, since it helps to maintain the stability of the conditionally stable integration methods, by keeping the high mode response of multi-degree-of freedom systems out of the solution.

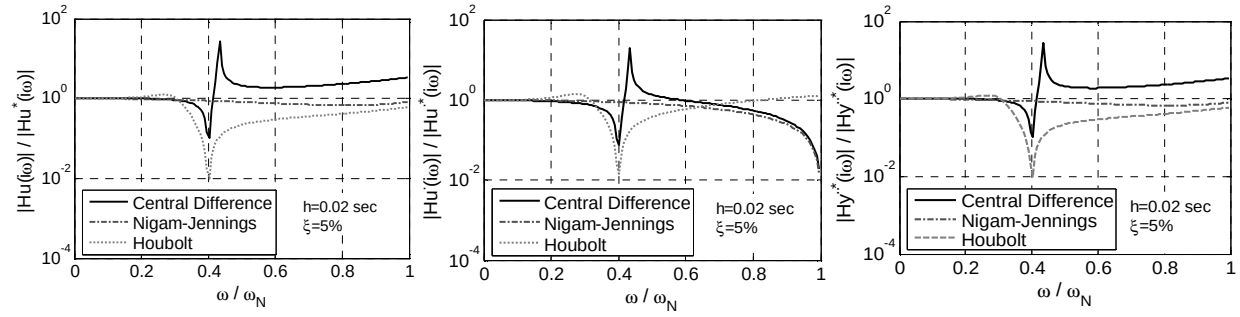

a) T_n = 0.1 sec.

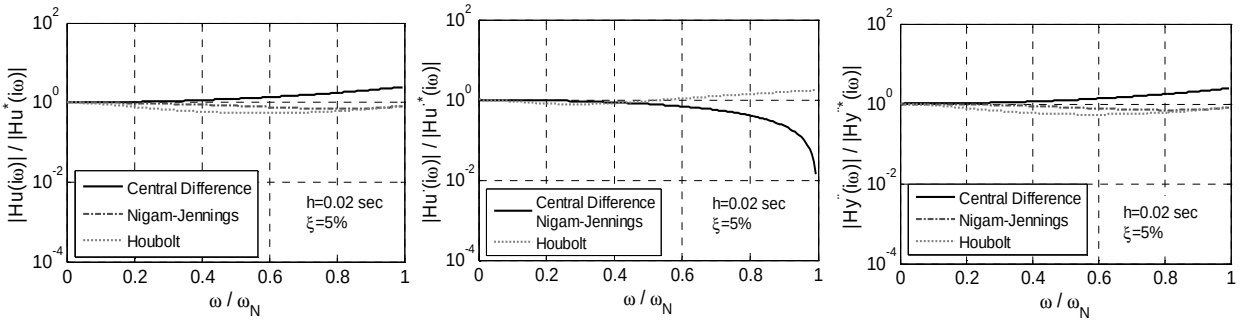

b) T_n = 5 sec.

Figure 9.- Normalized amplitude transfer function diagrams of three time stepping methods for short and long period 1 D.O.F. systems.

Fig 10 visualizes the normalized phase angles of the N-J, Houbolt and central difference methods. Attention is brought to the fact that Houbolt's method introduces a marked distortion in the phase angles of the response, since those angles become frequency-dependent. This feature is undesirable and may explain the poor accuracy of this method in solving certain dynamical problems.

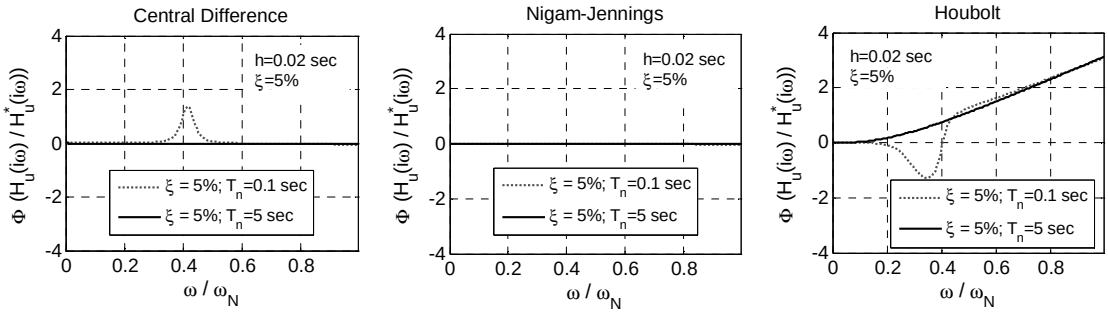

Figure 10.- Normalized displacement phase diagrams of three time stepping methods for short and long period 1 D.O.F. systems.

3.2. Response spectrum analysis

As explained before, all the integration schemes, even if they meet stability, convergence and consistency requirements, introduce numerical errors in the seismic response of 1 D.O.F. systems, which result in misleading response spectra. Fig. 11-b displays the peak errors of the response relative to the analytical absolute acceleration spectrum of the input record shown in Fig. 4-a. It can be seen that the accuracy errors on the forced vibration phase affect basically to the low periods, and should no be confused with the amplitude decay errors reported elsewhere (Humar, 1990) for the free vibration phase, that affect basically to long period systems. It is also observed that the Nigam-Jennings method and the 3rd order Runge-Kutta method (Heun's method) provide very similar results (Fig. 11-a). The 3rd order Runge-Kutta method, somehow less accurate and more costly in terms of computing time, was the standard for response spectra calculations prior to 1968 (Nigam and Jennings, 1969).

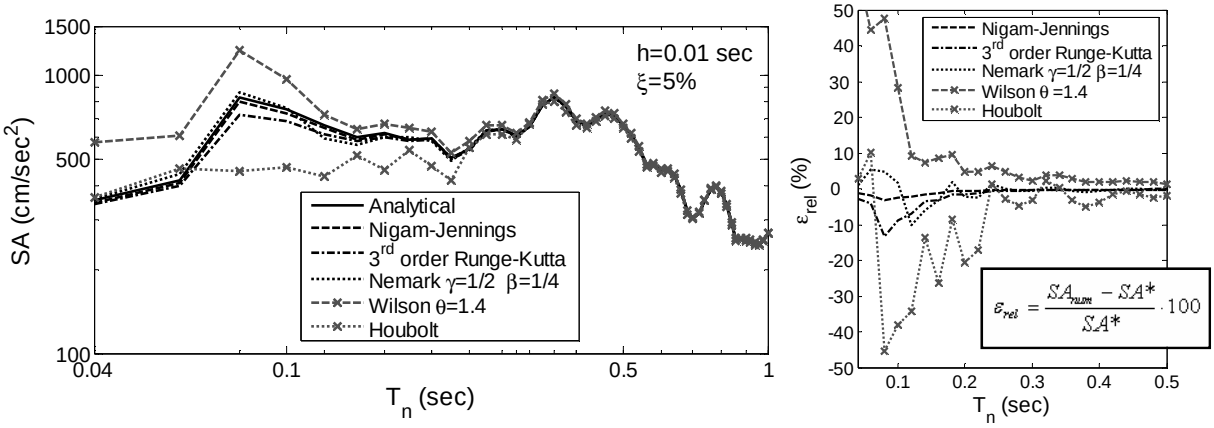

a) b)

Figure 11.- a) Numerical vs. analytical absolute acceleration spectra of the artificial accelerogram of Fig. 4-a; b) relative error of the numerical (approximate) spectrum ordinates with respect to the analytical (exact) values.

4. CONCLUSIONS

1) Algorithms that amplify significantly the upper half part of the Nyquist interval are very sensitive to the presence of spurious high frequency noise in seismic signals and should be avoided in dynamic response computations.

2) Phase shift in integration schemes distorts the frequency content and the shape of the excitation signals, introducing unacceptable drift errors in the integrated records.
3) In general, numerical transfer functions of 1 D.O.F. systems (especially short period systems) show a sharp peak at the resonance region of the oscillator, diverging considerably from the shape of the exact transfer curves in that zone.
4) Time-dependent Duhamel's transfer functions apply to the transient and stationary phases of the evolutionary seismic motions, while for step-by-step methods only the transfer functions of the stationary phases are computed.
5) Integration methods that introduce numerical damping in the response of the system filter out the high frequencies from the system's response. The truncation effect is very smooth and uniform for Nigam-Jennings method which deamplifies lightly the whole range of frequencies for all types of oscillators.
6) The amplitude of the integration interval is the main parameter controlling the stability and accuracy of seismic response of linear systems: the smaller the interval the greater the accuracy.

REFERENCES

Blázquez, R. (2007). Análisis frecuencial de los métodos de integración temporal en Ingeniería Sísmica. 3er Congreso Nacional de Ingeniería Sísmica, Girona, Spain, 1631-1655 (in Spanish).

Blázquez, R. and Arcos, A. (1999a). Numerical errors in the computation of Duhamel's integral. 2éme Rencontre en Génie Parasismique des Pays Méditerranéens (SISMICA 99), Faro, Portugal, 435-444.

Blázquez, R. and Arcos, A. (1999b). Transfer functions of time integration algorithms used in response spectrum analysis of earthquakes. Proceedings of the Fourth European Conference on Structural Dynamics (EURODYN'99), Prague, Czech Republic, 7-10 June, 1087-1093.

Bogdanoff, J.L., Godberg, J.E. and Bernard, M.C. (1961). Response of a simple structure to a random earthquake type disturbance. Bulletin of the Seismological Society of America, **51:2**, 293-310.

Hamming, R.W. (1977). Digital filters. Prentice-Hall International, Inc., Englewood Cliffs, N.J.

Humar, J.L. (1990). Dynamics of Structures. PrenticeHall, Englewood Cliffs, N.J.

Lin, Y.K. (1967). Probabilistic theory of structural dynamics. Mc Graw-Hill, Inc., New York.

Nigam, N.C. and Jennings, P.C. (1969). Calculation of response spectra from strong-motion earthquake records. Bulletin of the Seismological Society of America, **56:2**, 909-922.

Preumont, A. (1982). Frequency domain analysis of time integration operators. Earthquake Engineering and Structural Dynamics, **10**, 691-697.

ACKNOWLEDGEMENTS

The authors express their gratitude to the Ministry of Education and Science of Spain which provided grant and scholarship funding in support of this research (project BIA 2007-67401).